

## Diffusion weighted imaging: Technique and applications

Vinit Baliyan, Chandan J Das, Raju Sharma, Arun Kumar Gupta

Vinit Baliyan, Chandan J Das, Raju Sharma, Arun Kumar Gupta, Department of Radiology, All India Institute of Medical Sciences, New Delhi 110029, India

**Author contributions:** Baliyan V wrote the paper; Das CJ has designed and concepted the article; Sharma R and Gupta AK performed literature search and manuscript reviewing.

**Conflict-of-interest statement:** Authors declare no conflict of interests for this article.

**Open-Access:** This article is an open-access article which was selected by an in-house editor and fully peer-reviewed by external reviewers. It is distributed in accordance with the Creative Commons Attribution Non Commercial (CC BY-NC 4.0) license, which permits others to distribute, remix, adapt, build upon this work non-commercially, and license their derivative works on different terms, provided the original work is properly cited and the use is non-commercial. See: <http://creativecommons.org/licenses/by-nc/4.0/>

**Manuscript source:** Invited manuscript

**Correspondence to:** Chandan J Das, MD, Department of Radiology, All India Institute of Medical Sciences, Ansari Nagar, New Delhi 110029, India. [docchandan17@gmail.com](mailto:docchandan17@gmail.com)  
Telephone: +91-11-26593628  
Fax: +91-11-26588663

Received: February 29, 2016

Peer-review started: March 9, 2016

First decision: May 13, 2016

Revised: July 24, 2016

Accepted: August 11, 2016

Article in press: August 15, 2016

Published online: September 28, 2016

se evaluation and assessment of disease progression. Ability to detect and quantify the anisotropy of diffusion leads to a new paradigm called diffusion tensor imaging (DTI). DTI is a tool for assessment of the organs with highly organised fibre structure. DWI forms an integral part of modern state-of-art magnetic resonance imaging and is indispensable in neuroimaging and oncology. DWI is a field that has been undergoing rapid technical evolution and its applications are increasing every day. This review article provides insights in to the evolution of DWI as a new imaging paradigm and provides a summary of current role of DWI in various disease processes.

**Key words:** Diffusion weighted imaging; Diffusion tensor imaging; Onco-imaging; Neuro-imaging

© **The Author(s) 2016.** Published by Baishideng Publishing Group Inc. All rights reserved.

**Core tip:** Diffusion weighted imaging has revolutionised the magnetic resonance imaging. There is wide use of this technique in neuroimaging, body imaging as well as in oncoimaging. This article reviews the current role of diffusion weighted imaging in medical imaging and highlights the current challenges and limitations to this technique.

Baliyan V, Das CJ, Sharma R, Gupta AK. Diffusion weighted imaging: Technique and applications. *World J Radiol* 2016; 8(9): 785-798 Available from: URL: <http://www.wjgnet.com/1949-8470/full/v8/i9/785.htm> DOI: <http://dx.doi.org/10.4329/wjr.v8.i9.785>

### Abstract

Diffusion weighted imaging (DWI) is a method of signal contrast generation based on the differences in Brownian motion. DWI is a method to evaluate the molecular function and micro-architecture of the human body. DWI signal contrast can be quantified by apparent diffusion coefficient maps and it acts as a tool for treatment respon-

### INTRODUCTION

Approximately 60%-70% of the human body is composed of water. Diffusion is the random Brownian motion of the molecules driven by thermal energy. In a perfectly homogenous medium diffusion is random and isotropic; *i.e.*, equal probability in all directions. But in a complex environment of human body, water is divided

between cells and extracellular compartments. Water molecules in extracellular environments experience relatively free diffusion while intracellular molecules show relatively "restricted diffusion". Different tissues of the human body have a characteristic cellular architecture and proportions of intra and extracellular compartments; and hence have characteristic diffusion properties. The relative proportion of the water distribution between these compartments is affected by the pathologic processes. For example in high grade malignancies and acutely infarcted tissues, intracellular proportion is increased, so the diffusion becomes relatively more restricted. Diffusion weighted imaging provides qualitative and quantitative information about the diffusion properties. It adds a new dimension to the magnetic resonance imaging (MRI) examinations by adding functional information to the largely anatomical information gathered by the conventional sequences. Water diffusion is anisotropic in brain white matter, because axon membranes limit molecular movement perpendicular to the fibers. Diffusion tensor imaging (DTI) exploits this property to produce micro-architectural detail of white matter tracts and provides information about white matter integrity.

#### **Technical evolution of diffusion weighted imaging**

The goal of all imaging procedures is generation of an image contrast with a good spatial resolution. Initial evolution of diagnostic imaging focussed on tissue density function for signal contrast generation. In 1970s, the work of Lauterbur PC, Mansfield P and Ernst R, modern clinical MRI came into the field of medicine<sup>[1]</sup>. MRI provided an excellent contrast resolution not only from tissue (proton) density, but also from tissue relaxation properties. After initial focus on T1 and T2 relaxation properties researchers explored other methods to generate contrast exploiting other properties of water molecules. Diffusion weighted imaging (DWI) was a result of such efforts by researchers like Stejskal, Tanner and Le Bihan<sup>[2]</sup>.

In 1984, before MRI contrast became available, Denis Le Bihan, tried to differentiate liver tumors from angiomas. He hypothesized that a molecular diffusion measurement would result in low values for solid tumors, because of restriction of molecular movement. Based on the pioneering work of Stejskal and Tanner in the 1960s, he thought that diffusion encoding could be accomplished using specific magnetic gradient pulses. It was a challenging task to integrate the diffusion encoding gradients in to the conventional sequences and initial experience in the liver with a 0.5T scanner was very disappointing. Firstly diffusion MRI was a very slow method and it was very sensitive to motion artifacts due to respiration<sup>[2]</sup>.

It was not until the availability of Echo-Planar Imaging (EPI) in the early 1990s, that DWI could become a reality in the field of clinical imaging<sup>[2,3]</sup>. EPI based diffusion sequences were fast and solved the problems of motion artifacts. Early work by Moseley *et al*<sup>[4]</sup> and Warach *et*

*al*<sup>[5]</sup> established DWI as a cornerstone for early detection of acute stroke.

In a DWI sequence diffusion sensitization gradients are applied on either side of the 180° refocusing pulse. The parameter "b value" decides the diffusion weighting and is expressed in s/mm<sup>2</sup>. It is proportional to the square of the amplitude and duration of the gradient applied. Diffusion is qualitatively evaluated on trace images and quantitatively by the parameter called apparent diffusion coefficient (ADC). Tissues with restricted diffusion are bright on the trace image and hypointense on the ADC map.

#### **DTI evolution**

Moseley *et al*<sup>[4]</sup> observed that white matter contrast on diffusion images changes according to the spatial direction of the diffusion encoding gradients. Douek *et al*<sup>[6]</sup> suggested that this was due to the fact that water diffusion in white matter fibres was faster in the direction of the fibers and slower perpendicular to them, *i.e.*, anisotropic. The initial attempts were not very impressive, because diffusion measurements were done only along two directions. With the use of a tensor formalism by Basser *et al*<sup>[7]</sup> and development of 3D representation algorithms for fibre bundle depiction modern DTI came into existence. Initial clinical applications of DTI were limited to the central nervous system. Imaging artefacts and the small calibre of peripheral nerves hampered its use in the peripheral nervous system. However recent advances in MRI technology have extended its application to the peripheral nervous system<sup>[8]</sup>.

---

## **CLINICAL APPLICATIONS OF DWI**

---

### **Acute brain ischemia**

Ever since its inception acute brain ischemia has been the most successful application of DWI (Figure 1). Diffusion MRI today is the imaging modality of choice for stroke patients<sup>[9]</sup>. The use of DWI in combination with perfusion MRI, which outlines salvageable areas of ischemia and MR angiography, provides a useful guide for stroke management. The b-values up-to 1000 are used for standard neuroimaging application. Despite the historical success the interpretation of the molecular basis behind the diffusion restriction has been poorly understood. The relationship of diffusion restriction with the severity of the ischemia and the clinical outcome remains unresolved<sup>[10]</sup>.

### **Brain tumors**

ADC values have been shown to be decreased in highly cellular tumors such as CNS lymphoma, medulloblastoma, and high-grade glioma. Lower ADC values have been reported to be associated with higher-grades and poorer prognosis. Quantitative ADC measurements have also been helpful in prediction of therapeutic response. It is especially useful in detecting pseudo-response and pseudo-progression. Pseudo-response is a phenomenon seen after anti-angiogenic therapy where

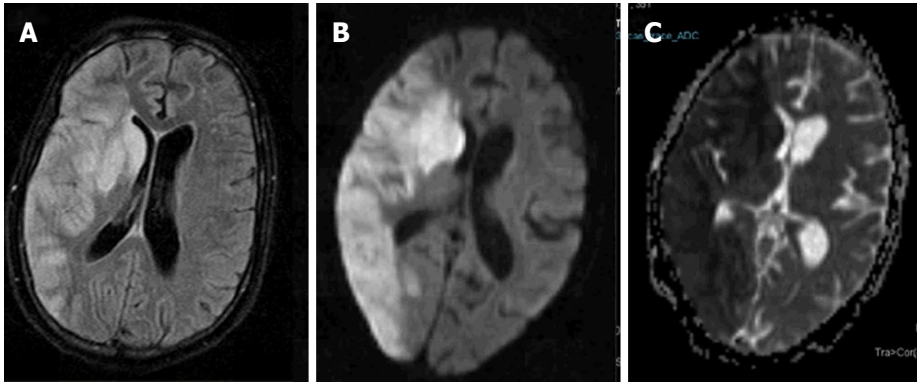


**Figure 1 Acute infarct.** Axial FLAIR image (A) shows geographic hyperintensity involving right parieto-occipital region and basal ganglia. Diffusion weighted imaging shows restricted diffusion with high signal on b1000 image (B) and low signal intensity on apparent diffusion coefficient map (C).

tumor doesn't enhance despite the intact viability or actual progression. DWI may be useful to demonstrate persistent or progressive tumor despite the lack of contrast enhancement. Pseudo-progression is seen in the setting of edema associated with the inflammatory response rather than progression of the true tumor. ADC values have been reported to be have an accuracy of up-to 80% in resolving the two entities<sup>[11]</sup>. DTI is helpful for intraoperative navigational purposes in order to avoid injuring the corticospinal tracts<sup>[12]</sup>.

#### White matter diseases

The exquisite sensitivity of DW MRI to microstructural changes enables us to detect the abnormalities much before changes on conventional images. In white matter, any change in tissue orientation patterns inside the MRI voxel results in a change in the degree of anisotropy and there is growing evidence in literature to support this assumption. Clinical studies carried on patients with white matter diseases have shown the sensitivity of DTI to detect abnormalities at an early stage and to demonstrate the microstructural abnormalities in various white matter diseases. Examples include multiple sclerosis, Alzheimer disease, leukoencephalopathies, Wallerian degeneration, Cerebral Autosomal Dominant Arteriopathy with Subcortical Infarcts and Leukoencephalopathy and HIV-1 encephalopathy<sup>[13-18]</sup>.

Anisotropy measurements may highlight more subtle anomalies in the organization of white matter tracks otherwise not visible on anatomical imaging. This property extends the potential of DTI in detecting more subtle changes, *e.g.*, functional disorders that do not necessarily have an anatomical basis. The potential is enormous and covers cognitive impairment, schizophrenia, dyslexia and various other psychiatric disorders<sup>[10]</sup>.

#### Pediatric brain development and aging

Brain's microstructure is not static, white matter tracts mature during early life and then degenerate with aging. Effects of aging on white matter organization have been studied<sup>[19,20]</sup>. DTI has a potential in the evaluation pediatric population. The degree of diffusion anisotropy in white matter increases during the myelination process

and hence water diffusion properties of white matter in the brain change dramatically during development. Diffusion metrics are isotropic in the adult brain cortex but there is a short time window of anisotropy. This transient anisotropy effect probably reflects the cellular migration and organization process within the cortical layers<sup>[10]</sup>. DTI can be used to monitor the myelination process during the different phases of development in fetuses, infants and childhood<sup>[20,21]</sup>. Similarly DTI can also be used to characterize white matter disorders and grey matter migration disorders in children<sup>[22,23]</sup>.

#### Oncological applications

Diffusion-weighted imaging has got immense potential in the field of onco-imaging. It is easy to implement and adds very little time to a standard MR examination. Malignant lesions have lower ADC values compared to surrounding normal tissue, edema and benign tumors in brain, head and neck malignancies, prostate and liver cancer<sup>[24]</sup>. Malignant tumors differ in their cellularity and biologic aggressiveness, which can be quantified in terms of ADC values<sup>[24,25]</sup>. Whole-body DWI, *i.e.*, diffusion weighted whole body imaging with background suppression (DWIBS) is performed using a STIR EPI sequence with a high *b* value for background suppression. Imaging is performed at multiple stations and then post-processed to form a composite image of the whole body. The images are displayed as maximum intensity projections with a reversed gray scale<sup>[26]</sup>. Signals from majority of normal tissue are suppressed with some exceptions such as the prostate, spleen, ovaries, testes, spinal cord and endometrium. Areas showing restricted diffusion such as highly cellular lymph nodes are strikingly highlighted. Small foci of tumors within the abdomen or peritoneum may also get highlighted by using this technique<sup>[26,27]</sup>. Recent applications of DWI in oncology include evaluation of response to chemoradiotherapy. Increase in ADC value can be detected before the size of the tumor decreases<sup>[28,29]</sup>.

#### Head and neck malignancies

DW-MRI has been applied in head and neck neoplasms (Figure 2). There is a significant difference in ADC

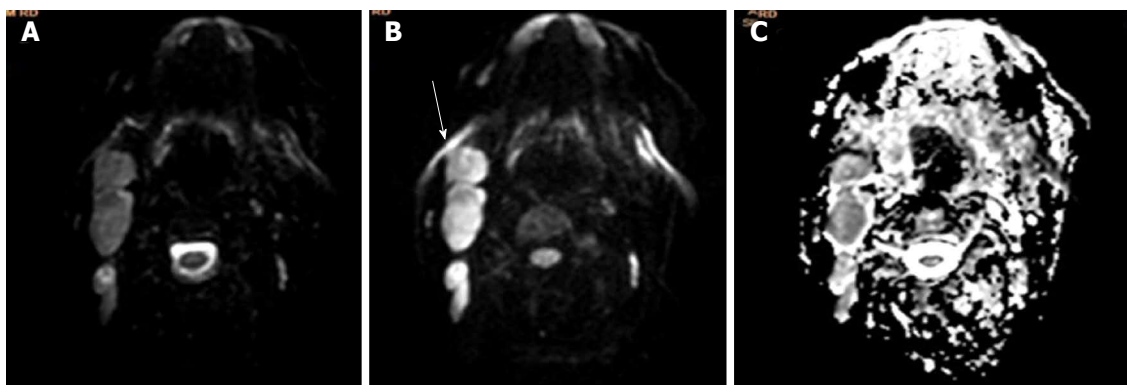


**Figure 2 Non-hodgkin's lymphoma.** Axial b0 (A), b1000 (B) and apparent diffusion coefficient map are showing multiple enlarged neck nodes. Nodes are showing slightly hyperintense signal on b0 images and retaining their signal on b1000 image with low signal on corresponding ADC (C). ADC: Apparent diffusion coefficient.

values of carcinomas, lymphomas, benign salivary gland tumors and benign cysts. Wang *et al.*<sup>[30]</sup> reported that ADC less than  $1.22 \times 10^{-3} \text{ mm}^2/\text{s}$  has 86% predictive accuracy for malignancy with 84% sensitivity and 91% specificity. DWI helps in the differentiation of benign from malignant tumors, lymphoma from squamous cell cancer, and benign from metastatic lymphadenopathy. It also helps in differentiation of necrotic tumors from abscesses and selection of appropriate site for biopsy. ADC value of necrosis is especially helpful in discriminating metastasis from lymphadenitis. Kato *et al.*<sup>[31]</sup> reported significantly lower ADC value in suppurative lymphadenitis ( $0.89 \pm 0.21$ ) than in malignancies ( $1.46 \pm 0.46$ ). In another study Zhang *et al.*<sup>[32]</sup> reported additional value of ADC measurements in necrotic and solid portions. ADC calculations are also useful in monitoring the patient after chemo-radiotherapy and differentiation of recurrent tumors from post-treatment changes<sup>[28,29,33,34]</sup>.

### Thoracic malignancies

DWI can be used for distinguishing malignant from benign and inflammatory lung lesions and helps in differentiation of small cell cancers (SCLC) from non-small cell cancers (NSCLC)<sup>[35,36]</sup>. In a recent meta-analysis by Shen *et al.*<sup>[35]</sup> reported that malignant pulmonary lesions have significantly lower ADC values than benign lesions [ $1.21$  (95%CI:  $1.19$ - $1.22$ )  $\text{mm}^2/\text{s}$  vs  $1.76$  (95%CI:  $1.72$ - $1.80$ )  $\text{mm}^2/\text{s}$ ]; and there is a significant difference between ADC values of small cell lung cancer and non-small cell lung cancer although differentiation of various histological subtypes were not possible<sup>[35,37]</sup>. Nomori *et al.*<sup>[38]</sup> showed that signal intensity and heterogeneity of DWI reflect the histologic heterogeneity and biological aggressiveness in NSCLC. DWI also has a high specificity in the lymph node staging of NSCLC<sup>[39]</sup>.

### Breast cancer

Using  $b$  values up-to  $400 \text{ s}/\text{mm}^2$ , Sinha *et al.*<sup>[40]</sup> reported that malignant breast lesions have significantly lower than the ADC values than benign diseases ( $1.36 \pm 0.36 \times 10^{-3}$  vs  $2.01 \pm 0.46 \times 10^{-3}$ ). It is now a routine part of multi-parametric MR evaluation of breast masses (Figure 3). Quantitative DTI measurements have been used as

an adjunct to dynamic contrast enhanced (DCE)-MRI. Wang *et al.*<sup>[41]</sup> have reported that compared to DCE-MRI used alone this strategy significantly improves the diagnostic performance of MRI for differential diagnosis between ductal carcinoma *in situ* (DCIS) and invasive breast cancer<sup>[42]</sup>. The sensitivity of the DTI parameters to detect breast cancer was found to be high, particularly in dense breasts.

### Hepatobiliary pancreatic cancers

DWI is helpful in focal liver lesion detection and characterization and can be used as an alternative to Gadolinium enhanced MRI in patients with renal dysfunction (Figures 4-7)<sup>[25]</sup>. Clinical applications of DW MRI include treatment response monitoring and prognostication in patients receiving systemic and focal ablative therapies for hepatic and pancreatic malignancies<sup>[43-46]</sup>. Hardie *et al.*<sup>[47]</sup> compared the utility of DWI in detection of liver metastases. They reported that DWI has 66.3% sensitivity compared to 73.5% for CE-MRI and hence it can serve as a useful alternative for this purpose. DW MR imaging has been investigated in diffuse hepatic parenchymal disease such as non-alcoholic fatty liver disease and hepatic fibrosis. However its clinical applicability is questionable as it suffers from multiple confounders making quantifying liver fibrosis through ADC difficult<sup>[48]</sup>. In a recent meta-analysis, Hong *et al.*<sup>[48]</sup> reported that DWI has a sensitivity and specificity of 0.83 (95%CI: 0.79-0.87) and 0.77 (95%CI: 0.70-0.83) for differentiation of malignant from benign pancreatic lesions. In another meta-analysis, Niu *et al.*<sup>[49]</sup> reported pooled sensitivity of 0.86 (95%CI: 0.80-0.91) and the pooled specificity of 0.82 (95%CI: 0.72-0.89) for differentiation of pancreatic carcinoma from mass-forming chronic pancreatitis. For most abdominal applications  $b$ -values of 0, 400 and 800 are standard except for prostate imaging where use of values up-to b1600 is considered more suitable.

### Bowel disorders

DWI is useful for detection of colorectal cancer, nodal and hepatic metastases and prediction of response after radio-chemotherapy for locally advanced rectal

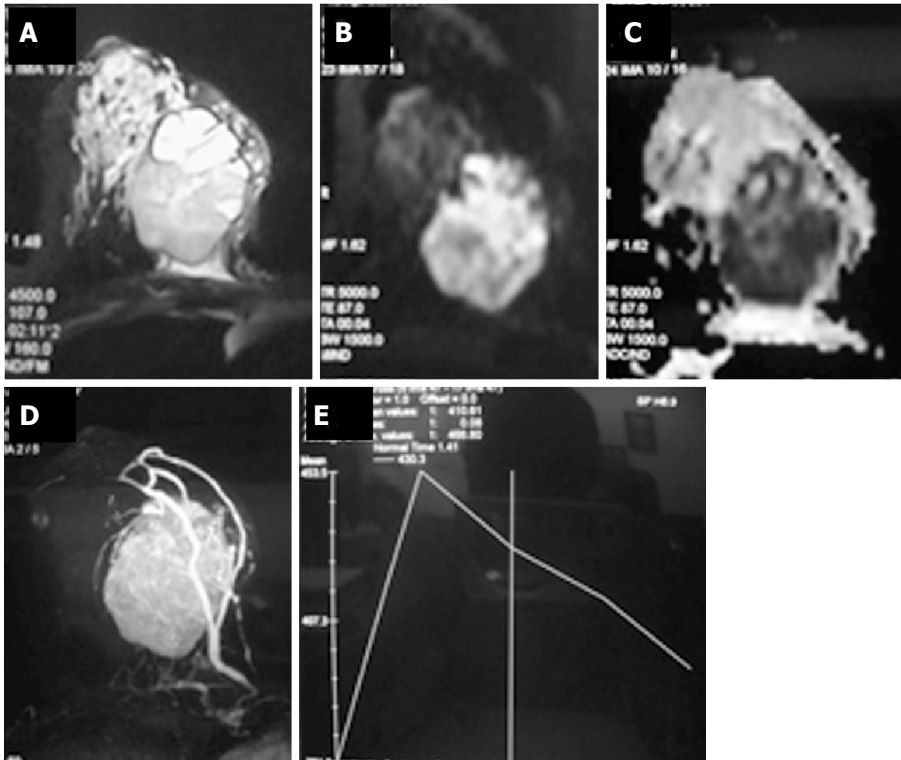


**Figure 3 Carcinoma breast.** Axial T2W fat saturated image (A) is showing a heterogeneously hyperintense mass lesion in right breast. Mass is showing hyperintense signal on b800 image (B), with low signal on apparent diffusion coefficient map (C); dynamic post-contrast MIP image (D) is showing contrast enhancement within the mass with type 3 enhancement curve (E).

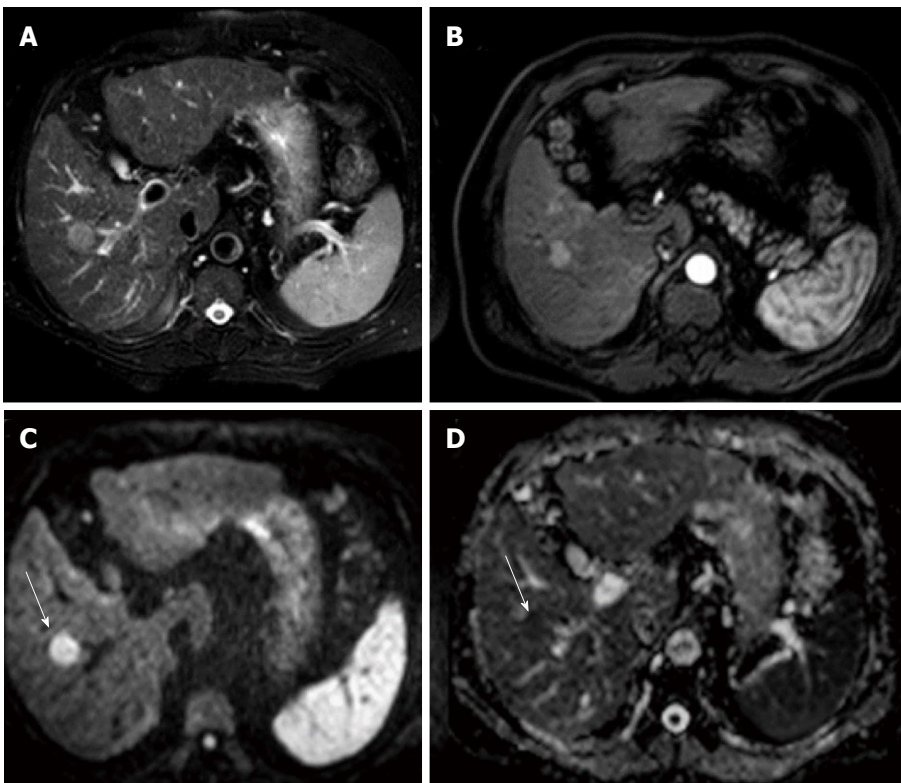


**Figure 4 Hepatocellular carcinoma in cirrhotic liver.** Axial T2W image is showing a hyperintense lesion in segment 5 of liver (A); lesion is enhancing in arterial phase (B); and it shows hyperintense signal on b800 image (C) and hypointense on apparent diffusion coefficient map (D).

cancer<sup>[50-52]</sup>. DWI detects therapy-induced modifications in lesion vascularity during anti-angiogenic therapy

before significant changes in size are evident<sup>[53,54]</sup>. DWIBS has been reported a useful tool in detection of

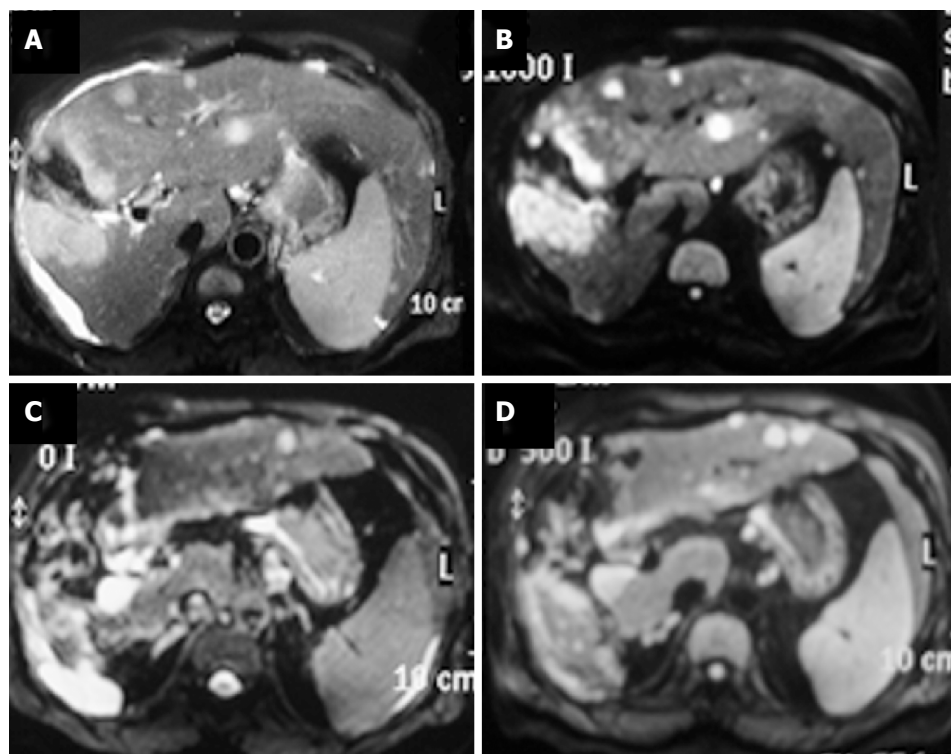


**Figure 5 Liver metastases.** Patient with gall bladder carcinoma is showing a large T2 hyperintense mass in gall bladder fossa (A) showing restricted diffusion on b1000 image (B); there are multiple metastatic lesions in liver in segments 2, 3 and 4. These lesions are also showing restricted diffusion. Another important point is the fact that a b500 image (D) is showing more lesion compared to a corresponding b0 image (C).

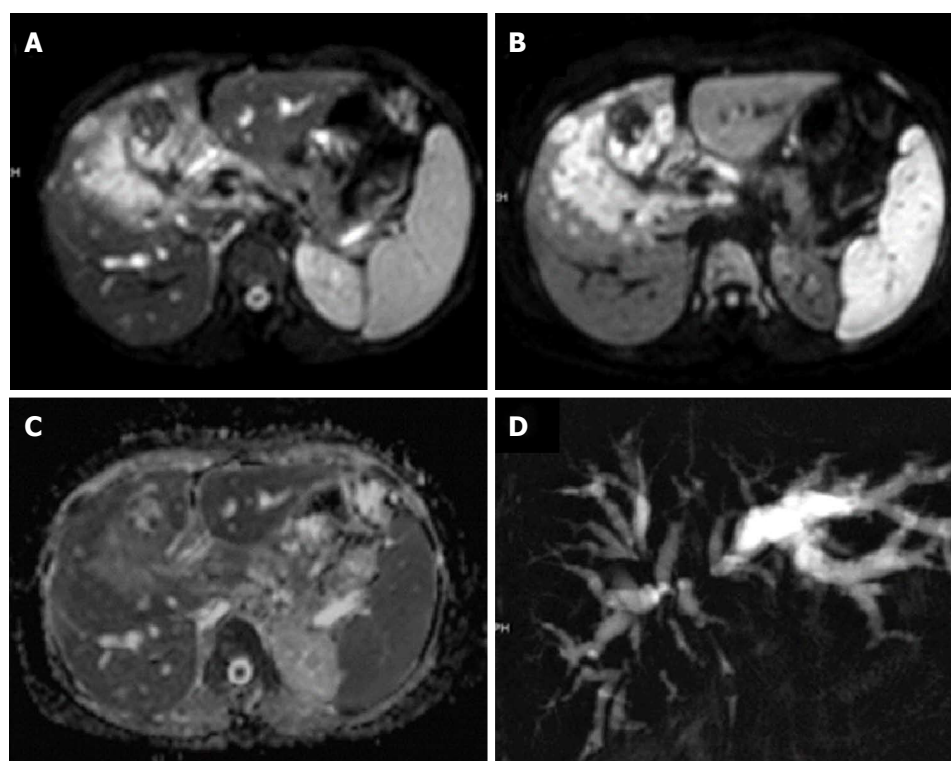


**Figure 6 Carcinoma gall bladder.** Axial T2W image showing a large heterogeneously hyperintense mass in gall bladder fossa of liver. It is showing hyperintense signal on b700 image (B) and are showing peripheral hyperintense signal on apparent diffusion coefficient map (C); coronal projectional MRCP image is showing biliary obstruction with involvement of primary and right secondary biliary confluence.

nodal metastasis of colorectal cancer<sup>[55]</sup>. In addition to its utility in abdominal malignancies, DWI has also been

found useful in inflammatory bowel disease. Qi *et al.*<sup>[56]</sup> reported that DWI combined with MR enterography

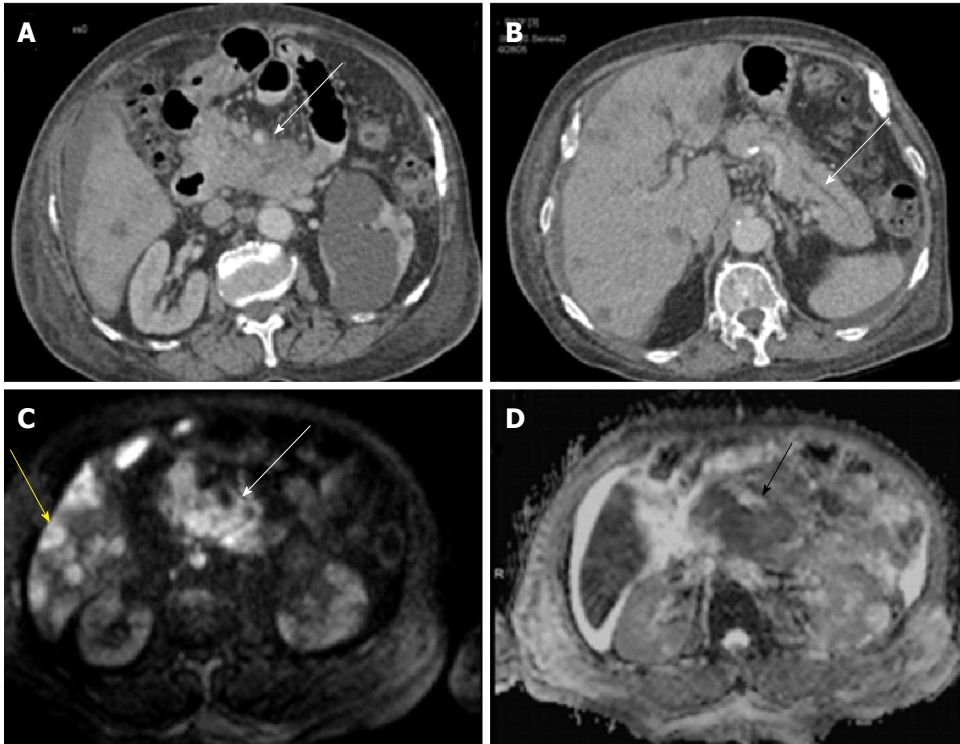


**Figure 7 Pancreatic adenocarcinoma.** Axial CECT images showing a hypo-enhancing mass in the neck and head region of pancreas (A) with a dilated pancreatic duct (B); multiple hypodense lesions can be noted within the liver parenchyma. Mass in the neck and head region of pancreas is showing hyperintense signal on b800 image and so are the focal liver lesions (C); corresponding apparent diffusion coefficient map shows hypointense signal within the mass (D).

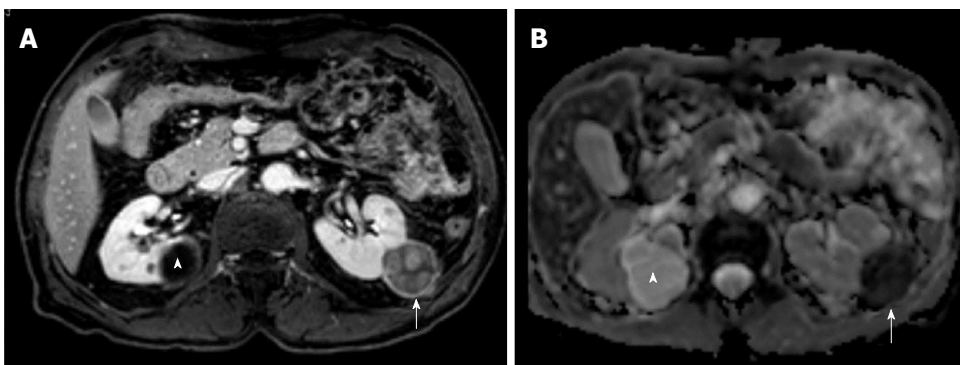


**Figure 8 Renal cell carcinoma vs simple cyst.** Axial contrast-enhanced magnetic resonance image shows non-enhancing bosniak category I cyst in right kidney (arrowhead) and Bosniak category IV cyst (enhancing mural nodules) in left kidney (arrow). Former shows free diffusion with high ADC while latter depicts restricted diffusion with low ADCs. Latter was found to be clear cell renal cell carcinoma. ADC: Apparent diffusion coefficient.

(MRE) has higher diagnostic accuracy (92%) than MRE alone (79%) for disease activity. It has also been found to be useful in detection and characterization of extraintestinal manifestations and complications<sup>[57]</sup>. Use of DWI with MR enterography improves mesenteric and small bowel tumor detection compared to unenhanced MR-enterography<sup>[58]</sup>.

**Genito-urinary applications**

DWI can easily distinguish benign renal cysts from solid neoplasms (Figures 8 and 9)<sup>[59]</sup>. There have been attempts to distinguish various histological subtypes, but due to overlap in the ADC values such predictions have been found to be difficult<sup>[59-61]</sup>. In patients with

transitional cell cancer, histological grade is the most important factor determining biological aggressiveness. ADC values correlate very well with histopathological grades of TCC, and hence predict the biological behaviour of bladder cancer and tumour recurrence (Figures 10 and 11)<sup>[59]</sup>. DWI helps to detect carcinoma in the transition zone and increases the diagnostic confidence in detection of peripheral zone cancer (Figure 12). DWIBS is useful in detection of skeletal metastasis (Figure 13)<sup>[59]</sup>.

DWI improves the diagnosis of cervical and endometrial tumors<sup>[62]</sup>. DW MR imaging is especially useful for accurate determination of the depth of myometrial invasion in patients with endometrial cancer<sup>[63]</sup>. It has

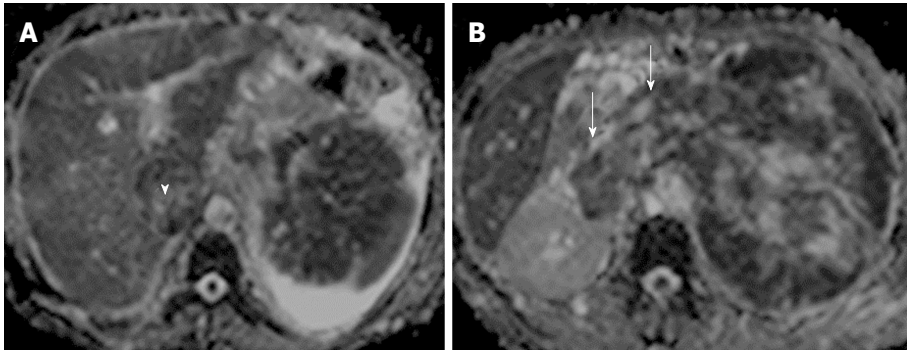


**Figure 9 Renal cell carcinoma with malignant inferior vena cava thrombus.** Apparent diffusion coefficient maps (A and B) of a patient with large left renal mass with contiguous extension into renal vein (arrows) and inferior vena cava (arrowhead) (malignant thrombosis). Both the renal mass and intravascular thrombus had similar apparent diffusion coefficient values.

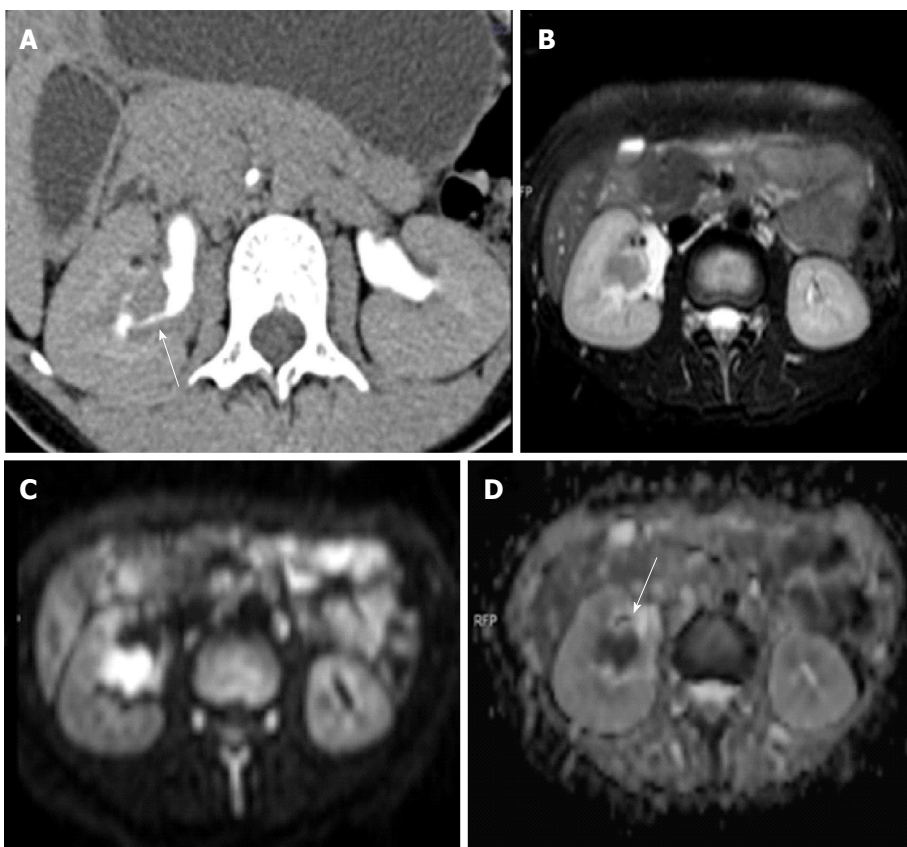


**Figure 10 Transitional cell cancer.** Computed tomography urography image (A) shows a filling defect within the mid-pole calyx and infundibular region. Axial T2W image (B) showing a corresponding hypointense lesion showing restricted diffusion on diffusion weighted imaging (C, D).

also been suggested to be a potential response biomarker in cervical cancer<sup>[64]</sup>. DWI is highly sensitive for detection of peritoneal dissemination in gynecological malignancy and plays an important role in the management of gynecological malignancies especially ovarian cancer (Figure 11)<sup>[65]</sup>. ADC changes have also been shown to be useful in prediction of uterine leiomyoma volume response after uterine artery embolization<sup>[66]</sup>, preoperative differentiation between uterine leiomyoma and leiomyosarcoma<sup>[67]</sup>.

### Peripheral nerve imaging

Advancements in DTI technology have expanded

its application to peripheral nervous system (Figure 14). DTI adds value to conventional MR Neurography as it is capable of axonal and myelin compartment differentiation. DTI parameters "axial diffusivity" and "fractional anisotropy" are considered as markers of axon integrity and myelin sheath integrity respectively. DTI has been used to quantitatively evaluate spinal nerve entrapment with foraminal stenosis. The entrapped roots and distal spinal nerve show increased diffusivity and significantly lower FA values than the normal nerves<sup>[68,69]</sup>. DTI has also been studied in animal models for monitoring peripheral nerve degeneration and regeneration<sup>[70]</sup>. The experience of DTI in nerve imaging is

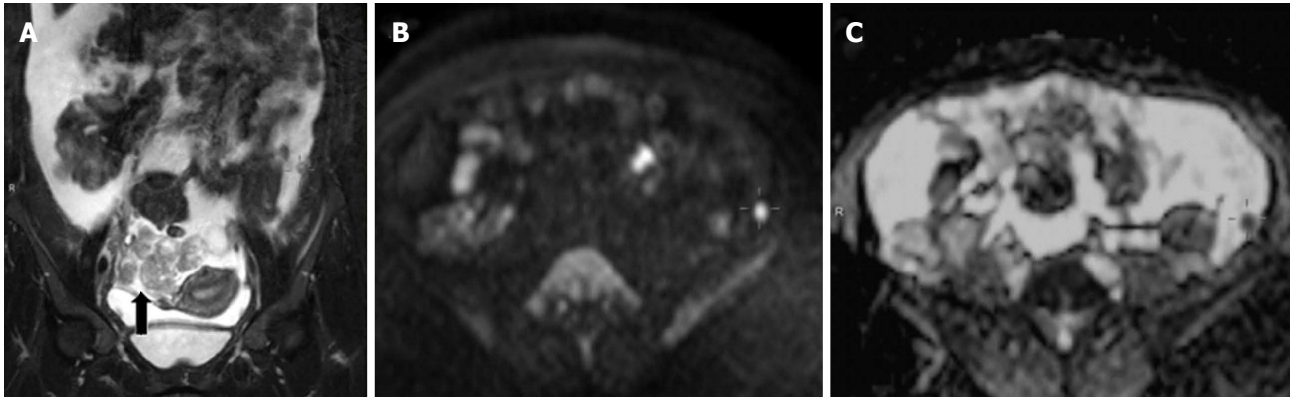


**Figure 11 Carcinoma ovary.** Coronal T2W image shows right adnexal mass with gross ascitis (A); B800 image (B) showing a focal hyperintense peritoneal nodule in left iliac fossa region with corresponding dark signal on apparent diffusion coefficient map (C).

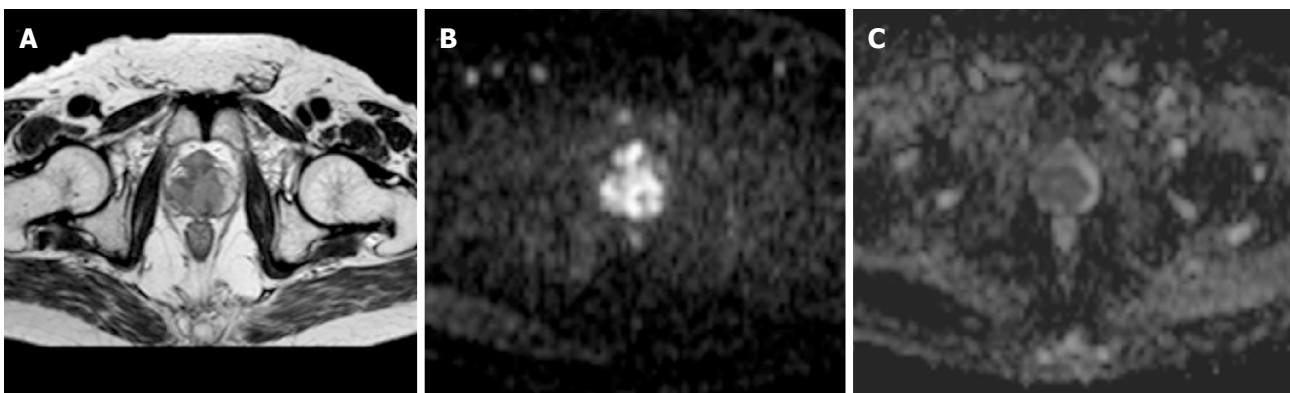


**Figure 12 Carcinoma prostate.** Axial T2W image (A) showing central T2 corresponding hypointensity on apparent diffusion coefficient map (C) and high signal on b1000 image (B) suggesting a central gland prostate cancer.

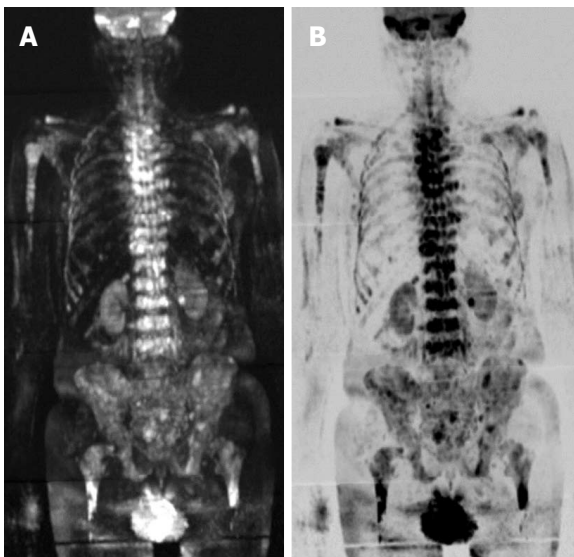


**Figure 13 Carcinoma prostate metastases.** DWIBS images showing multiple metastatic lesions within the vertebral bodies, pelvic bones, B/L proximal femur and humerus.

limited and it is yet to achieve its full potential<sup>[71]</sup>.

### Musculoskeletal applications

DWI improves diagnostic accuracy of MR imaging in

the differentiation of acute osteoporotic from malignant compression fractures (Figure 15)<sup>[72]</sup>. Structural integrity of the spinal cord can be assessed by DTI. Quantitative analysis of anisotropy and diffusivity detects subtle abnormalities that can be easily missed on conventional imaging. DTI has been found to be useful tool in various conditions involving spinal cord. Such conditions include spinal cord injury, multiple sclerosis, amyotrophic lateral sclerosis, myelitis, and spinal cord tumors<sup>[73]</sup>.

### LIMITATIONS

The algorithms used in DWI acquisition make several assumptions, *e.g.*, perfect field homogeneity, infinitely fast gradient changes, and perfectly shaped RF pulses, *etc.* However, with the available technology, the gradient coils can generate gradient magnitudes and switch rate of the order of  $40 \text{ mTm}^{-1}$  and  $200 \text{ Tm}^{-1}\cdot\text{s}^{-1}$  respectively. Such discrepancies limit DWI accuracy and result in lower image quality and image artifacts<sup>[74]</sup>. Major limitations of DWI are experienced in body imaging and are largely because of it being an EPI sequence<sup>[59,60]</sup>. DWI is susceptible to various artifacts, *e.g.*, T2 shine through, T2 black out, ghosting, blurring and distortions. Tissues with very long relaxation times might tend to retain signal on high *b* value images. This is known as "T2

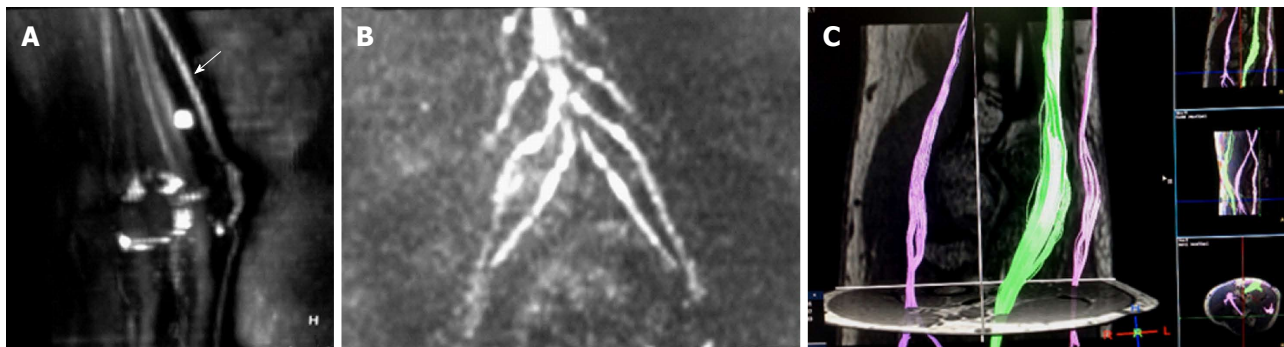


**Figure 14** Diffusion tensor imaging images. It shows ulnar nerve (A) and sacral plexus (B); (C) is showing diffusion tensor imaging of nerve fibers of nerves around elbow.

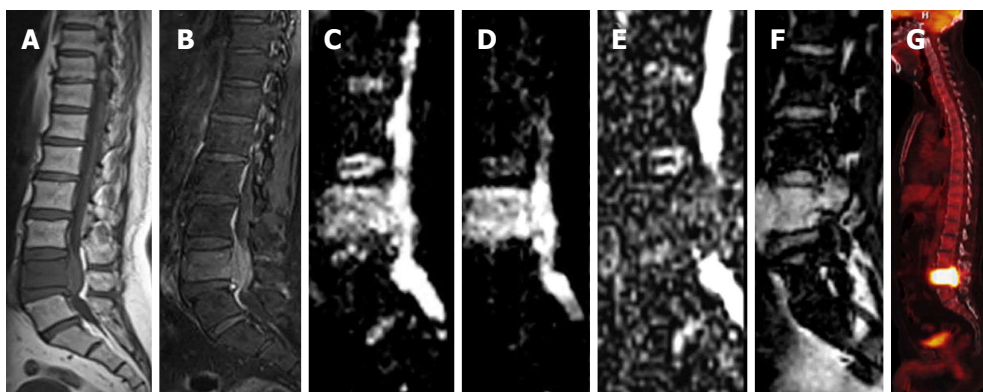


**Figure 15** Vertebral metastasis. Sagittal T1W image (A) is showing diffuse T2 hypointense signal within the L5 vertebral body with corresponding hyperintense signal and associated prevertebral and extradural soft tissue on STIR image (B). Diffusion weighted imaging images (C, D) are showing hyperintense signal with low signal on apparent diffusion coefficient map (E). There is contrast enhancement within the involved vertebra (F) and intense uptake on positron emission tomography image (G).

shine through” effect. Corresponding bright signal on ADC map by such lesions helps to differentiate it from restricted diffusion, which appears dark on ADC maps. T2 blackout effect is the term used for low signal on ADC map due to lack of enough water protons and not due to restricted diffusion. Low signal on T2 weighted fat saturated images is the diagnostic sign for such an effect.

Image quality provided by single shot EPI is limited and has a low spatial resolution and a poor SNR. 3T MRI has an inherent high SNR, but presents several limitations as well. Susceptibility artifacts are more pronounced at 3T and uniform fat suppression is also a challenge with 3 Tesla magnets<sup>[75]</sup>. Parallel imaging technique improves SNR by allowing a decrease in TE<sup>[76]</sup>.

Another bothersome limitation of DWI is the questionable reproducibility of ADC values. ADC values can vary even with the use of same MR system. Such variability has been attributed to the inherent low SNR, artifacts and distortions related to SS EPI sequence. Rapid on/off transition of diffusion gradients during EPI sequence causes eddy-current related distortions resulting in image degradation and systemic errors in ADC calculations<sup>[77]</sup>.

## ADDRESSING CURRENT CHALLENGES AND FUTURE DIRECTIONS

Most of the challenges encountered during DWI acquisitions can be minimized by optimizing the DW-MR protocol. Researchers have been focusing on further optimization of DWI sequences and have been making new advancements to enhance the utility of DWI. Non-EPI sequences (turbo-FLASH, HASTE, SSFP) or dual-source parallel RF excitation DWI are novel strategies to overcome the disadvantages of 3T systems<sup>[78,79]</sup>. Periodically rotated overlapping parallel lines with enhanced reconstruction technique based on the fast spin echo (FSE) sequence has been used for DWI acquisitions to nullify the geometric distortion of EPI<sup>[80]</sup>. It is of advantage in temporal bone and spinal cord imaging<sup>[81]</sup>. “TRacking Only Navigator echo” (TRON) is a new acquisition technique for DWI to address the motion related distortions. It allows continuous real-time slice tracking and position correction without use of any kind of gating<sup>[82]</sup>. Refocused spin echo preparation (bipolar EPI sequence) is an emerging approach to minimize distortions related to the eddy currents<sup>[83]</sup>. Fast advanced

spin-echo sequence DWI has been reported to be more sensitive and/or accurate than those obtained with EPI-DWI for N-stage assessments of NSCLC patients<sup>[84]</sup>. Intravoxel incoherent motion with bi-exponential diffusion model is a method of harnessing perfusion information from diffusion acquisitions<sup>[27]</sup>. Routine DW imaging assumes that water in biological environment follows Gaussian laws (normal distribution), which is an oversimplification. Actually water molecules in such environments have non-gaussian properties that can be quantified by diffusion kurtosis imaging (DKI). DKI provides a measure of tissue heterogeneity and indicate the complexity of the microstructural environment. It provides complementary information to that acquired with traditional diffusion imaging and may lead to broadening of DWI applications<sup>[85]</sup>.

Recent work in the field of diffusion MRI has focused on its application to study the function of brain. Until recently positron emission tomography (PET) and functional BOLD MRI have been used for measurement of brain activity. Le Bihan *et al.*<sup>[86]</sup> have shown that water diffusion properties are modulated by the brain activity. The changes on diffusion functional MRI are faster than the changes with BOLD functional MRI, which measure the reactive increase in blood flow<sup>[87]</sup>. The introduction of diffusion functional MRI has opened a new paradigm. It has got huge potential for resolving complex mysteries of neurophysiology.

## CONCLUSION

DWI has become an indispensable imaging tool. It has well established roles in the fields of stroke imaging, white matter diseases and oncology. While conventional imaging provided only anatomical information, DWI has opened a new paradigm with information about molecular activity and cellular function. Recent advances in this field have touched new horizons with the arrival of functional diffusion MRI. Researchers believe that DWI has still not achieved to its full potential and it is expected that in future DWI may be able to solve the most complex puzzles of brain functioning.

## REFERENCES

- 1 **Geva T.** Magnetic resonance imaging: historical perspective. *J Cardiovasc Magn Reson* 2006; **8**: 573-580 [PMID: 16869310]
- 2 **Le Bihan D.** Diffusion MRI: what water tells us about the brain. *EMBO Mol Med* 2014; **6**: 569-573 [PMID: 24705876 DOI: 10.1002/emmm.201404055]
- 3 **Turner R,** Le Bihan D, Maier J, Vavrek R, Hedges LK, Pekar J. Echo-planar imaging of intravoxel incoherent motion. *Radiology* 1990; **177**: 407-414 [PMID: 2217777 DOI: 10.1148/radiology.177.2.2217777]
- 4 **Moseley ME,** Cohen Y, Mintorovitch J, Chileuitt L, Shimizu H, Kucharczyk J, Wendland MF, Weinstein PR. Early detection of regional cerebral ischemia in cats: comparison of diffusion- and T2-weighted MRI and spectroscopy. *Magn Reson Med* 1990; **14**: 330-346 [PMID: 2345513]
- 5 **Warach S,** Chien D, Li W, Ronthal M, Edelman RR. Fast magnetic resonance diffusion-weighted imaging of acute human stroke. *Neurology* 1992; **42**: 1717-1723 [PMID: 1513459]
- 6 **Doek P,** Turner R, Pekar J, Patronas N, Le Bihan D. MR color mapping of myelin fiber orientation. *J Comput Assist Tomogr* 1991; **15**: 923-929 [PMID: 1939769]
- 7 **Basser PJ,** Mattiello J, LeBihan D. MR diffusion tensor spectroscopy and imaging. *Biophys J* 1994; **66**: 259-267 [PMID: 8130344 DOI: 10.1016/S0006-3495(94)80775-1]
- 8 **Naraghi AM,** Awdeh H, Wadhwa V, Andreisek G, Chhabra A. Diffusion tensor imaging of peripheral nerves. *Semin Musculoskelet Radiol* 2015; **19**: 191-200 [PMID: 25764243 DOI: 10.1055/s-0035-1546824]
- 9 **Chalela JA,** Kidwell CS, Nentwich LM, Luby M, Butman JA, Demchuk AM, Hill MD, Patronas N, Latour L, Warach S. Magnetic resonance imaging and computed tomography in emergency assessment of patients with suspected acute stroke: a prospective comparison. *Lancet* 2007; **369**: 293-298 [PMID: 17258669 DOI: 10.1016/S0140-6736(07)60151-2]
- 10 **Le Bihan D,** Johansen-Berg H. Diffusion MRI at 25: exploring brain tissue structure and function. *Neuroimage* 2012; **61**: 324-341 [PMID: 22120012 DOI: 10.1016/j.neuroimage.2011.11.006]
- 11 **Lee WJ,** Choi SH, Park CK, Yi KS, Kim TM, Lee SH, Kim JH, Sohn CH, Park SH, Kim IH. Diffusion-weighted MR imaging for the differentiation of true progression from pseudoprogression following concomitant radiotherapy with temozolomide in patients with newly diagnosed high-grade gliomas. *Acad Radiol* 2012; **19**: 1353-1361 [PMID: 22884399 DOI: 10.1016/j.acra.2012.06.011]
- 12 **Mabray MC,** Barajas RF, Cha S. Modern brain tumor imaging. *Brain Tumor Res Treat* 2015; **3**: 8-23 [PMID: 25977902 DOI: 10.14791/btr.2015.3.1.8]
- 13 **Chabriat H,** Pappata S, Poupon C, Clark CA, Vahedi K, Poupon F, Mangin JF, Pachot-Clouard M, Jobert A, Le Bihan D, Bousser MG. Clinical severity in CADASIL related to ultrastructural damage in white matter: in vivo study with diffusion tensor MRI. *Stroke* 1999; **30**: 2637-2643 [PMID: 10582990]
- 14 **Eichler FS,** Itoh R, Barker PB, Mori S, Garrett ES, van Zijl PC, Moser HW, Raymond GV, Melhem ER. Proton MR spectroscopic and diffusion tensor brain MR imaging in X-linked adrenoleukodystrophy: initial experience. *Radiology* 2002; **225**: 245-252 [PMID: 12355012 DOI: 10.1148/radiol.2251011040]
- 15 **Hanyu H,** Sakurai H, Iwamoto T, Takasaki M, Shindo H, Abe K. Diffusion-weighted MR imaging of the hippocampus and temporal white matter in Alzheimer's disease. *J Neurol Sci* 1998; **156**: 195-200 [PMID: 9588857]
- 16 **Werring DJ,** Clark CA, Barker GJ, Thompson AJ, Miller DH. Diffusion tensor imaging of lesions and normal-appearing white matter in multiple sclerosis. *Neurology* 1999; **52**: 1626-1632 [PMID: 10331689]
- 17 **Horsfield MA,** Larsson HB, Jones DK, Gass A. Diffusion magnetic resonance imaging in multiple sclerosis. *J Neurol Neurosurg Psychiatry* 1998; **64** Suppl 1: S80-S84 [PMID: 9647291]
- 18 **Filippi CG,** Ulug AM, Ryan E, Ferrando SJ, van Gorp W. Diffusion tensor imaging of patients with HIV and normal-appearing white matter on MR images of the brain. *AJNR Am J Neuroradiol* 2001; **22**: 277-283 [PMID: 11156769]
- 19 **Moseley M.** Diffusion tensor imaging and aging - a review. *NMR Biomed* 2002; **15**: 553-560 [PMID: 12489101 DOI: 10.1002/nbm.785]
- 20 **Pfefferbaum A,** Sullivan EV, Hedehus M, Lim KO, Adalsteinsson E, Moseley M. Age-related decline in brain white matter anisotropy measured with spatially corrected echo-planar diffusion tensor imaging. *Magn Reson Med* 2000; **44**: 259-268 [PMID: 10918325]
- 21 **Dubois J,** Hertz-Pannier L, Dehaene-Lambertz G, Cointepas Y, Le Bihan D. Assessment of the early organization and maturation of infants' cerebral white matter fiber bundles: a feasibility study using quantitative diffusion tensor imaging and tractography. *Neuroimage* 2006; **30**: 1121-1132 [PMID: 16413790 DOI: 10.1016/j.neuroimage.2005.11.022]
- 22 **Takahashi M,** Ono J, Harada K, Maeda M, Hackney DB. Diffusional anisotropy in cranial nerves with maturation: quantitative evaluation with diffusion MR imaging in rats. *Radiology* 2000; **216**:

- 881-885 [PMID: 10966726 DOI: 10.1148/radiology.216.3.r00se418 81]
- 23 **Engelbrecht V**, Scherer A, Rassek M, Witsack HJ, Mödder U. Diffusion-weighted MR imaging in the brain in children: findings in the normal brain and in the brain with white matter diseases. *Radiology* 2002; **222**: 410-418 [PMID: 11818607 DOI: 10.1148/radiol.2222010492]
- 24 **Charles-Edwards EM**, deSouza NM. Diffusion-weighted magnetic resonance imaging and its application to cancer. *Cancer Imaging* 2006; **6**: 135-143 [PMID: 17015238 DOI: 10.1102/1470-7330.2006.0021]
- 25 **Chan JH**, Tsui EY, Luk SH, Fung AS, Yuen MK, Szeto ML, Cheung YK, Wong KP. Diffusion-weighted MR imaging of the liver: distinguishing hepatic abscess from cystic or necrotic tumor. *Abdom Imaging* 2001; **26**: 161-165 [PMID: 11178693]
- 26 **Takahara T**, Imai Y, Yamashita T, Yasuda S, Nasu S, Van Cauteren M. Diffusion weighted whole body imaging with background body signal suppression (DWIBS): technical improvement using free breathing, STIR and high resolution 3D display. *Radiat Med* 2004; **22**: 275-282 [PMID: 15468951]
- 27 **Koh DM**, Collins DJ, Orton MR. Intravoxel incoherent motion in body diffusion-weighted MRI: reality and challenges. *AJR Am J Roentgenol* 2011; **196**: 1351-1361 [PMID: 21606299 DOI: 10.2214/AJR.10.5515]
- 28 **Schouten CS**, de Graaf P, Alberts FM, Hoekstra OS, Comans EF, Bloemena E, Witte BI, Sanchez E, Leemans CR, Castelijns JA, de Bree R. Response evaluation after chemoradiotherapy for advanced nodal disease in head and neck cancer using diffusion-weighted MRI and 18F-FDG-PET-CT. *Oral Oncol* 2015; **51**: 541-547 [PMID: 25725587 DOI: 10.1016/j.oraloncology.2015.01.017]
- 29 **Varoquaux A**, Rager O, Dulguerov P, Burkhardt K, Ailianou A, Becker M. Diffusion-weighted and PET/MR Imaging after Radiation Therapy for Malignant Head and Neck Tumors. *Radiographics* 2015; **35**: 1502-1527 [PMID: 26252192 DOI: 10.1148/rg.2015140029]
- 30 **Wang J**, Takashima S, Takayama F, Kawakami S, Saito A, Matsushita T, Momose M, Ishiyama T. Head and neck lesions: characterization with diffusion-weighted echo-planar MR imaging. *Radiology* 2001; **220**: 621-630 [PMID: 11526259 DOI: 10.1148/radiol.2202010063]
- 31 **Kato H**, Kanematsu M, Kato Z, Teramoto T, Mizuta K, Aoki M, Makita H, Kato K. Necrotic cervical nodes: usefulness of diffusion-weighted MR imaging in the differentiation of suppurative lymphadenitis from malignancy. *Eur J Radiol* 2013; **82**: e28-e35 [PMID: 22954412 DOI: 10.1016/j.ejrad.2012.08.014]
- 32 **Zhang Y**, Chen J, Shen J, Zhong J, Ye R, Liang B. Apparent diffusion coefficient values of necrotic and solid portion of lymph nodes: differential diagnostic value in cervical lymphadenopathy. *Clin Radiol* 2013; **68**: 224-231 [PMID: 22316593 DOI: 10.1016/j.crad.2011.04.002]
- 33 **Razek AA**. Diffusion-weighted magnetic resonance imaging of head and neck. *J Comput Assist Tomogr* 2010; **34**: 808-815 [PMID: 21084893 DOI: 10.1097/RCT.0b013e3181f01796]
- 34 **Şerifoğlu İ**, Oz İİ, Damar M, Tokgöz Ö, Yazgan Ö, Erdem Z. Diffusion-weighted imaging in the head and neck region: usefulness of apparent diffusion coefficient values for characterization of lesions. *Diagn Interv Radiol* 2015; **21**: 208-214 [PMID: 25910284 DOI: 10.5152/dir.2014.14279]
- 35 **Shen G**, Jia Z, Deng H. Apparent diffusion coefficient values of diffusion-weighted imaging for distinguishing focal pulmonary lesions and characterizing the subtype of lung cancer: a meta-analysis. *Eur Radiol* 2016; **26**: 556-566 [PMID: 26003791 DOI: 10.1007/s00330-015-3840-y]
- 36 **Deng Y**, Li X, Lei Y, Liang C, Liu Z. Use of diffusion-weighted magnetic resonance imaging to distinguish between lung cancer and focal inflammatory lesions: a comparison of intravoxel incoherent motion derived parameters and apparent diffusion coefficient. *Acta Radiol* 2015 May 13; Epub ahead of print [PMID: 25972370 DOI: 10.1177/0284185115586091]
- 37 **Liu LP**, Zhang XX, Cui LB, Li J, Yang JL, Yang HN, Zhang Y, Zhou Y, Tang X, Qi S, Fang Y, Zhang J, Yin H. Preliminary comparison of diffusion-weighted MRI and PET/CT in predicting histological type and malignancy of lung cancer. *Clin Respir J* 2015 Apr 27; Epub ahead of print [PMID: 25918835 DOI: 10.1111/crj.12316]
- 38 **Nomori H**, Cong Y, Abe M, Sugimura H, Kato Y. Diffusion-weighted magnetic resonance imaging in preoperative assessment of non-small cell lung cancer. *J Thorac Cardiovasc Surg* 2015; **149**: 991-996 [PMID: 25686657 DOI: 10.1016/j.jtcvs.2015.01.019]
- 39 **Zhang Y**, Qin Q, Li B, Wang J, Zhang K. Magnetic resonance imaging for N staging in non-small cell lung cancer: A systematic review and meta-analysis. *Thorac Cancer* 2015; **6**: 123-132 [PMID: 26273348 DOI: 10.1111/1759-7714.12203]
- 40 **Sinha S**, Lucas-Quesada FA, Sinha U, DeBruhl N, Bassett LW. In vivo diffusion-weighted MRI of the breast: potential for lesion characterization. *J Magn Reson Imaging* 2002; **15**: 693-704 [PMID: 12112520 DOI: 10.1002/jmri.10116]
- 41 **Wang Y**, Zhang X, Cao K, Li Y, Li X, Qi L, Tang L, Wang Z, Gao S. Diffusion-tensor imaging as an adjunct to dynamic contrast-enhanced MRI for improved accuracy of differential diagnosis between breast ductal carcinoma in situ and invasive breast carcinoma. *Chin J Cancer Res* 2015; **27**: 209-217 [PMID: 25937784 DOI: 10.3978/j.issn.1000-9604.2015.03.04]
- 42 **Nissan N**, Furman-Haran E, Feinberg-Shapiro M, Grobgeld D, Eyal E, Zehavi T, Degani H. Tracking the mammary architectural features and detecting breast cancer with magnetic resonance diffusion tensor imaging. *J Vis Exp* 2014; **(94)** [PMID: 25549209 DOI: 10.3791/52048]
- 43 **De Robertis R**, Tinazzi Martini P, Demozzi E, Puntel G, Ortolani S, Cingolini S, Ruzzenente A, Guglielmi A, Tortora G, Bassi C, Pederzoli P, D'Onofrio M. Prognostication and response assessment in liver and pancreatic tumors: The new imaging. *World J Gastroenterol* 2015; **21**: 6794-6808 [PMID: 26078555 DOI: 10.3748/wjg.v21.i22.6794]
- 44 **Cuneo KC**, Chenevert TL, Ben-Josef E, Feng MU, Greenon JK, Hussain HK, Simeone DM, Schipper MJ, Anderson MA, Zalupski MM, Al-Hawary M, Galban CJ, Rehemtulla A, Feng FY, Lawrence TS, Ross BD. A pilot study of diffusion-weighted MRI in patients undergoing neoadjuvant chemoradiation for pancreatic cancer. *Transl Oncol* 2014; **7**: 644-649 [PMID: 25389460 DOI: 10.1016/j.tranon.2014.07.005]
- 45 **Kurosawa J**, Tawada K, Mikata R, Ishihara T, Tsuyuguchi T, Saito M, Shimofusa R, Yoshitomi H, Ohtsuka M, Miyazaki M, Yokosuka O. Prognostic relevance of apparent diffusion coefficient obtained by diffusion-weighted MRI in pancreatic cancer. *J Magn Reson Imaging* 2015; **42**: 1532-1537 [PMID: 25946483 DOI: 10.1002/jmri.24939]
- 46 **Mannelli L**, Bhargava P, Osman SF, Raz E, Moshiri M, Laffi G, Wilson GJ, Maki JH. Diffusion-weighted imaging of the liver: a comprehensive review. *Curr Probl Diagn Radiol* 2013; **42**: 77-83 [PMID: 23683849 DOI: 10.1067/j.cpradiol.2012.07.001]
- 47 **Hardie AD**, Naik M, Hecht EM, Chandarana H, Mannelli L, Babb JS, Taouli B. Diagnosis of liver metastases: value of diffusion-weighted MRI compared with gadolinium-enhanced MRI. *Eur Radiol* 2010; **20**: 1431-1441 [PMID: 20148251 DOI: 10.1007/s00330-009-1695-9]
- 48 **Hong BZ**, Li XF, Lin JQ. Differential diagnosis of pancreatic cancer by single-shot echo-planar imaging diffusion-weighted imaging. *World J Gastroenterol* 2015; **21**: 6374-6380 [PMID: 26034373 DOI: 10.3748/wjg.v21.i20.6374]
- 49 **Niu X**, Das SK, Bhetuwal A, Xiao Y, Sun F, Zeng L, Wang W, Yang H, Yang H. Value of diffusion-weighted imaging in distinguishing pancreatic carcinoma from mass-forming chronic pancreatitis: a meta-analysis. *Chin Med J (Engl)* 2014; **127**: 3477-3482 [PMID: 25269917]
- 50 **Ichikawa T**, Erturk SM, Motosugi U, Sou H, Iino H, Araki T, Fujii H. High-B-value diffusion-weighted MRI in colorectal cancer. *AJR Am J Roentgenol* 2006; **187**: 181-184 [PMID: 16794174 DOI: 10.2214/AJR.05.1005]
- 51 **Joye I**, Deroose CM, Vandecaveye V, Haustermans K. The role of diffusion-weighted MRI and (18)F-FDG PET/CT in the prediction

- of pathologic complete response after radiochemotherapy for rectal cancer: a systematic review. *Radiother Oncol* 2014; **113**: 158-165 [PMID: 25483833 DOI: 10.1016/j.radonc.2014.11.026]
- 52 **Meng X**, Huang Z, Wang R, Yu J. Prediction of response to preoperative chemoradiotherapy in patients with locally advanced rectal cancer. *Biosci Trends* 2014; **8**: 11-23 [PMID: 24647108]
- 53 **Anzidei M**, Napoli A, Zaccagna F, Cartocci G, Saba L, Menichini G, Cavallo Marincola B, Marotta E, Di Mare L, Catalano C, Passariello R. Liver metastases from colorectal cancer treated with conventional and antiangiogenic chemotherapy: evaluation with liver computed tomography perfusion and magnetic resonance diffusion-weighted imaging. *J Comput Assist Tomogr* 2011; **35**: 690-696 [PMID: 22082538 DOI: 10.1097/RCT.0b013e318230d905]
- 54 **Heijmen L**, Ter Voert EE, Nagtegaal ID, Span P, Bussink J, Punt CJ, de Wilt JH, Sweep FC, Heerschap A, van Laarhoven HW. Diffusion-weighted MR imaging in liver metastases of colorectal cancer: reproducibility and biological validation. *Eur Radiol* 2013; **23**: 748-756 [PMID: 23001604 DOI: 10.1007/s00330-012-2654-4]
- 55 **Shuto K**, Saito H, Ohira G, Miyauchi H, Matsubara H. Diffusion weighted whole body imaging with background body signal suppression (DWIBS) in nodal metastasis of colorectal cancer. *Nihon Rinsho* 2011; **69** Suppl 3: 315-319 [PMID: 22213976]
- 56 **Qi F**, Jun S, Qi QY, Chen PJ, Chuan GX, Jiong Z, Rong XJ. Utility of the diffusion-weighted imaging for activity evaluation in Crohn's disease patients underwent magnetic resonance enterography. *BMC Gastroenterol* 2015; **15**: 12 [PMID: 25653007 DOI: 10.1186/s12876-015-0235-0]
- 57 **Morani AC**, Smith EA, Ganeshan D, Dillman JR. Diffusion-weighted MRI in pediatric inflammatory bowel disease. *AJR Am J Roentgenol* 2015; **204**: 1269-1277 [PMID: 26001238 DOI: 10.2214/AJR.14.13359]
- 58 **Amzallag-Bellenger E**, Soyer P, Barbe C, Nguyen TL, Amara N, Hoeffel C. Diffusion-weighted imaging for the detection of mesenteric small bowel tumours with Magnetic Resonance-enterography. *Eur Radiol* 2014; **24**: 2916-2926 [PMID: 25113647 DOI: 10.1007/s00330-014-3303-x]
- 59 **Baliyan V**, Das CJ, Sharma S, Gupta AK. Diffusion-weighted imaging in urinary tract lesions. *Clin Radiol* 2014; **69**: 773-782 [PMID: 24581968 DOI: 10.1016/j.crad.2014.01.011]
- 60 **Koh DM**, Collins DJ. Diffusion-weighted MRI in the body: applications and challenges in oncology. *AJR Am J Roentgenol* 2007; **188**: 1622-1635 [PMID: 17515386 DOI: 10.2214/AJR.06.1403]
- 61 **Goyal A**, Sharma R, Bhalla AS, Gamanagatti S, Seth A, Iyer VK, Das P. Diffusion-weighted MRI in renal cell carcinoma: a surrogate marker for predicting nuclear grade and histological subtype. *Acta Radiol* 2012; **53**: 349-358 [PMID: 22496427 DOI: 10.1258/ar.2011.110415]
- 62 **Levy A**, Medjhouli A, Caramella C, Zareski E, Berges O, Chargari C, Boulet B, Bidault F, Dromain C, Balleyguier C. Interest of diffusion-weighted echo-planar MR imaging and apparent diffusion coefficient mapping in gynecological malignancies: a review. *J Magn Reson Imaging* 2011; **33**: 1020-1027 [PMID: 21509857 DOI: 10.1002/jmri.22546]
- 63 **Manoharan D**, Das CJ, Aggarwal A, Gupta AK. Diffusion weighted imaging in gynecological malignancies - present and future. *World J Radiol* 2016; **8**: 288-297 [PMID: 27027614 DOI: 10.4329/wjr.v8.i3.288]
- 64 **Makino H**, Kato H, Furui T, Morishige K, Kanematsu M. Predictive value of diffusion-weighted magnetic resonance imaging during chemoradiotherapy for uterine cervical cancer. *J Obstet Gynaecol Res* 2014; **40**: 1098-1104 [PMID: 24320754 DOI: 10.1111/jog.12276]
- 65 **Fujii S**, Matsusue E, Kanasaki Y, Kanamori Y, Nakanishi J, Sugihara S, Kigawa J, Terakawa N, Ogawa T. Detection of peritoneal dissemination in gynecological malignancy: evaluation by diffusion-weighted MR imaging. *Eur Radiol* 2008; **18**: 18-23 [PMID: 17701040 DOI: 10.1007/s00330-007-0732-9]
- 66 **Cao MQ**, Suo ST, Zhang XB, Zhong YC, Zhuang ZG, Cheng JJ, Chi JC, Xu JR. Entropy of T2-weighted imaging combined with apparent diffusion coefficient in prediction of uterine leiomyoma volume response after uterine artery embolization. *Acad Radiol* 2014; **21**: 437-444 [PMID: 24594413 DOI: 10.1016/j.acra.2013.12.007]
- 67 **Sato K**, Yuasa N, Fujita M, Fukushima Y. Clinical application of diffusion-weighted imaging for preoperative differentiation between uterine leiomyoma and leiomyosarcoma. *Am J Obstet Gynecol* 2014; **210**: 368.e1-368.e8 [PMID: 24368137 DOI: 10.1016/j.ajog.2013.12.028]
- 68 **Eguchi Y**, Ohtori S, Yamashita M, Yamauchi K, Suzuki M, Orita S, Kamoda H, Arai G, Ishikawa T, Miyagi M, Ochiai N, Kishida S, Masuda Y, Ochi S, Kikawa T, Takaso M, Aoki Y, Toyone T, Suzuki T, Takahashi K. Clinical applications of diffusion magnetic resonance imaging of the lumbar foraminal nerve root entrapment. *Eur Spine J* 2010; **19**: 1874-1882 [PMID: 20632042 DOI: 10.1007/s00586-010-1520-9]
- 69 **Chen YY**, Lin XF, Zhang F, Zhang X, Hu HJ, Wang DY, Lu LJ, Shen J. Diffusion tensor imaging of symptomatic nerve roots in patients with cervical disc herniation. *Acad Radiol* 2014; **21**: 338-344 [PMID: 24361075 DOI: 10.1016/j.acra.2013.11.005]
- 70 **Takagi T**, Nakamura M, Yamada M, Hikishima K, Momoshima S, Fujiyoshi K, Shibata S, Okano HJ, Toyama Y, Okano H. Visualization of peripheral nerve degeneration and regeneration: monitoring with diffusion tensor tractography. *Neuroimage* 2009; **44**: 884-892 [PMID: 18948210 DOI: 10.1016/j.neuroimage.2008.09.022]
- 71 **Heckel A**, Weiler M, Xia A, Ruetters M, Pham M, Bendszus M, Heiland S, Baeumer P. Peripheral Nerve Diffusion Tensor Imaging: Assessment of Axon and Myelin Sheath Integrity. *PLoS One* 2015; **10**: e0130833 [PMID: 26114630 DOI: 10.1371/journal.pone.0130833]
- 72 **Sung JK**, Jee WH, Jung JY, Choi M, Lee SY, Kim YH, Ha KY, Park CK. Differentiation of acute osteoporotic and malignant compression fractures of the spine: use of additive qualitative and quantitative axial diffusion-weighted MR imaging to conventional MR imaging at 3.0 T. *Radiology* 2014; **271**: 488-498 [PMID: 24484060 DOI: 10.1148/radiol.13130399]
- 73 **Bosma R**, Stroman PW. Diffusion tensor imaging in the human spinal cord: development, limitations, and clinical applications. *Crit Rev Biomed Eng* 2012; **40**: 1-20 [PMID: 22428796]
- 74 **Chilla GS**, Tan CH, Xu C, Poh CL. Diffusion weighted magnetic resonance imaging and its recent trend-a survey. *Quant Imaging Med Surg* 2015; **5**: 407-422 [PMID: 26029644 DOI: 10.3978/j.issn.2223-4292.2015.03.01]
- 75 **Rosenkrantz AB**, Oei M, Babb JS, Niver BE, Taouli B. Diffusion-weighted imaging of the abdomen at 3.0 Tesla: image quality and apparent diffusion coefficient reproducibility compared with 1.5 Tesla. *J Magn Reson Imaging* 2011; **33**: 128-135 [PMID: 21182130 DOI: 10.1002/jmri.22395]
- 76 **Bammer R**, Keeling SL, Augustin M, Pruessmann KP, Wolf R, Stollberger R, Hartung HP, Fazekas F. Improved diffusion-weighted single-shot echo-planar imaging (EPI) in stroke using sensitivity encoding (SENSE). *Magn Reson Med* 2001; **46**: 548-554 [PMID: 11550248]
- 77 **Sasaki M**, Yamada K, Watanabe Y, Matsui M, Ida M, Fujiwara S, Shibata E. Variability in absolute apparent diffusion coefficient values across different platforms may be substantial: a multivendor, multi-institutional comparison study. *Radiology* 2008; **249**: 624-630 [PMID: 18936317 DOI: 10.1148/radiol.2492071681]
- 78 **Dietrich O**, Biffar A, Baur-Melnyk A, Reiser MF. Technical aspects of MR diffusion imaging of the body. *Eur J Radiol* 2010; **76**: 314-322 [PMID: 20299172 DOI: 10.1016/j.ejrad.2010.02.018]
- 79 **Willinek WA**, Gieseke J, Kukuk GM, Nelles M, König R, Morakkabati-Spitz N, Träber F, Thomas D, Kuhl CK, Schild HH. Dual-source parallel radiofrequency excitation body MR imaging compared with standard MR imaging at 3.0 T: initial clinical experience. *Radiology* 2010; **256**: 966-975 [PMID: 20720078 DOI: 10.1148/radiol.10092127]
- 80 **Deng J**, Omary RA, Larson AC. Multishot diffusion-weighted SPLICE PROPELLER MRI of the abdomen. *Magn Reson Med* 2008; **59**: 947-953 [PMID: 18429036 DOI: 10.1002/mrm.21525]
- 81 **Karandikar A**, Loke SC, Goh J, Yeo SB, Tan TY. Evaluation of cholesteatoma: our experience with DW Propeller imaging. *Acta Radiol* 2015; **56**: 1108-1112 [PMID: 25260417 DOI: 10.1177/0284

- 185114549568]
- 82 **Takahara T**, Kwee TC, Van Leeuwen MS, Ogino T, Horie T, Van Cauteren M, Herigault G, Imai Y, Mali WP, Luijten PR. Diffusion-weighted magnetic resonance imaging of the liver using tracking only navigator echo: feasibility study. *Invest Radiol* 2010; **45**: 57-63 [PMID: 20057318 DOI: 10.1097/RLI.0b013e3181cc25ed]
- 83 **Kyriazi S**, Blackledge M, Collins DJ, Desouza NM. Optimising diffusion-weighted imaging in the abdomen and pelvis: comparison of image quality between monopolar and bipolar single-shot spin-echo echo-planar sequences. *Eur Radiol* 2010; **20**: 2422-2431 [PMID: 20711734 DOI: 10.1007/s00330-010-1826-3]
- 84 **Ohno Y**, Koyama H, Yoshikawa T, Takenaka D, Kassai Y, Yui M, Matsumoto S, Sugimura K. Diffusion-weighted MR imaging using FASE sequence for 3T MR system: Preliminary comparison of capability for N-stage assessment by means of diffusion-weighted MR imaging using EPI sequence, STIR FASE imaging and FDG PET/CT for non-small cell lung cancer patients. *Eur J Radiol* 2015; **84**: 2321-2331 [PMID: 26231045 DOI: 10.1016/j.ejrad.2015.07.019]
- 85 **Steven AJ**, Zhuo J, Melhem ER. Diffusion kurtosis imaging: an emerging technique for evaluating the microstructural environment of the brain. *AJR Am J Roentgenol* 2014; **202**: W26-W33 [PMID: 24370162 DOI: 10.2214/AJR.13.11365]
- 86 **Le Bihan D**, Urayama S, Aso T, Hanakawa T, Fukuyama H. Direct and fast detection of neuronal activation in the human brain with diffusion MRI. *Proc Natl Acad Sci USA* 2006; **103**: 8263-8268 [PMID: 16702549 DOI: 10.1073/pnas.0600644103]
- 87 **Tsurugizawa T**, Ciobanu L, Le Bihan D. Water diffusion in brain cortex closely tracks underlying neuronal activity. *Proc Natl Acad Sci USA* 2013; **110**: 11636-11641 [PMID: 23801756 DOI: 10.1073/pnas.1303178110]

**P- Reviewer:** Kilickesmez O, Lassandro F, Shen J, Theodorou K, Tirumani S **S- Editor:** Qiu S **L- Editor:** A **E- Editor:** Wu HL





Published by **Baishideng Publishing Group Inc**

8226 Regency Drive, Pleasanton, CA 94588, USA

Telephone: +1-925-223-8242

Fax: +1-925-223-8243

E-mail: [bpgoffice@wjgnet.com](mailto:bpgoffice@wjgnet.com)

Help Desk: <http://www.wjgnet.com/esps/helpdesk.aspx>

<http://www.wjgnet.com>

